DESIGN OF INJECTOR SYSTEMS FOR LUX *

S. Lidia#, LBNL, 1 Cyclotron Road, Berkeley, CA 94720 USA

Abstract

The LUX concept [1] for a superconducting recirculating linac based ultrafast x-ray facility features a unique high-brightness electron beam injector. The design of the injector complex that meets the baseline requirements for LUX is presented. A dual-rf gun injector provides both high-brightness electron beams to drive the cascaded, seeded harmonic generation VUV-soft x-ray FELs as well as the ultra- low-vertical emittance ('flat') beams that radiate in hard x-ray spontaneous emission synchrotron beamlines. Details of the injector complex design and performance characteristics are presented. Contributions by the thermal emittance and optical pulse shaping to the beam emission at the photocathode and to the beam dynamics throughout the injector are presented. Techniques that seek to optimize the injector performance, as well as constraints that prevent straightforward optimization, are discussed.

INTRODUCTION

The LUX concept for an ultrafast x-ray facility features a recirculating linac that accepts bright electron beams generated with a dual rf gun photoinjector [1]. The nominal design parameters for the injector complex have been previously discussed [2]. A schematic for the dual injector complex is depicted in Figure 1.

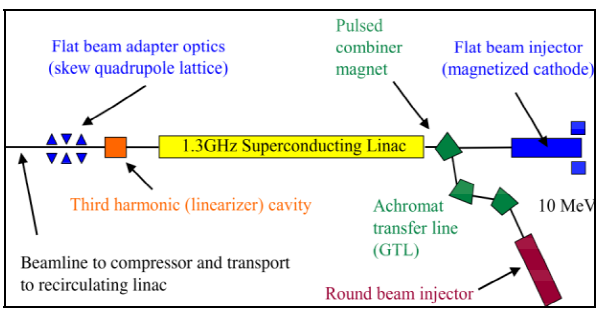

Figure 1. LUX dual photoinjector complex.

Two rf guns are necessary to produce two classes of beams. The (off-axis) 'round'-beam injector produces low emittance (< 2π mm-mrad) beams to drive VUV-soft x-ray FELs. The (on-axis) 'flat'-beam injector produces low emittance (< 3π mm-mrad) beams from a magnetized cathode (B_z ~ 0.1-1.0 kG). The angular momentum carried by the 'flat' beam is then used in the downstream adapter optics to create a beam with low vertical emittance (< 0.3π mm-mrad) and large x/y emittance ratio [3] to drive hard x-ray spontaneous emission devices. Both magnetized and unmagnetized beams carry a nominal 1 nC charge within a 30-35ps core. These two beams have separate transport beamlines from the cathodes to the entrance of the linac, but are then merged onto the same beamline for acceleration. The adapter and matching beamlines include pulsed skew and normal quadrupole magnets to produce uncoupled beams with identical beta functions at the entrance to the compressor.

*This work was supported by the Department of Energy, Office of Science under Contract No. DE_AC03-76SF00098.
#SMLidia@lbl.gov

RF GUN AND LINAC OPTIMIZATION

The design of the rf photoinjectors was presented previously [4]. Each four-cavity rf gun was optimized to produce minimum emittance beams at the gun exit with a combination of rf cavity phase and solenoid magnet settings, for an exit energy of ~10 MeV. The gradient profile of the individual cavities in the nine-cavity linac was adjusted to provide a balance of acceleration and transverse ponderomotive focusing for both the 'round' and 'flat' beams. The 3rd harmonic cavities at the linac exit are excited to remove 2nd order nonlinearities in the longitudinal phase space and to apply a tailored linear slope in preparation for compression.

Emittance Compensation

The emittance of beams with coupling of the transverse phase spaces is conserved in linear systems if one considers the total ('4D') emittance, $\varepsilon_{4D} = \varepsilon_r^2 + \varepsilon_L^2$, where ε_r is the radial emittance, and $\varepsilon_L = \sqrt{\left(\langle L^2\rangle - \langle L\rangle^2\right)/4}$ is the angular emittance for beams carrying average ($\langle L\rangle$) and RMS canonical angular momentum ($\sqrt{\langle L^2\rangle}$). All emittances are normalized and angular momenta are normalized to longitudinal momentum. The '4D' emittance can be expressed in the usual 2D units via $\varepsilon_{2D} = \sqrt{\varepsilon_{4D}}$. For uncoupled beams, $\varepsilon_{2D} = \sqrt{\varepsilon_x \varepsilon_y}$.

The strategy for emittance compensation for coupled beams was outlined previously [2]. Once the linac gradients were set, the gun-to-linac (GTL) drifts and the final rf gun solenoids were then adjusted to match the beam RMS envelopes as well as the phase of the transverse emittance oscillation so that a minimum spot size and transverse emittance are obtained at the linac exit. Figure 2 shows the result of this process for the two classes of beams using ASTRA [5]. Beams at the cathodes were generated with a uniform, 4mm diameter spot (σ_r=1mm), and 1.1π mm-mrad thermal emittance [6]. The incident laser pulse carries a uniform, temporal flat-top (35ps) with linearly ramped rise and fall times (2.5ps). A charge of 1nC is carried within the 35ps core. For the purpose of this design study, the achromatic transfer line for the 'round' beam was simply represented as a straight drift section. Future work will investigate the effects of the dipoles.

The optimization found minima in the 2D emittance

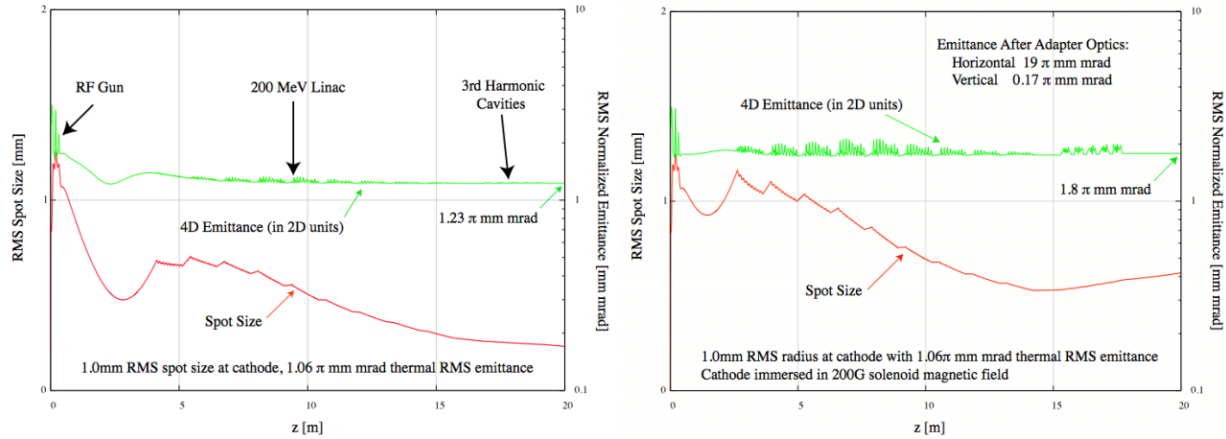

Figure 2. RMS emittance (2D) and spot size evolution (σ_r) from photocathode to the exit of the 3rd harmonic cavities for 'round' beams (left) and 'flat' beams (right). The emittance is projected over the 35ps, 1nC beam core.

at the linac exit which, while within the nominal specification for the injector, differed between the 'round' and 'flat' beams. This is not unexpected since the emittance compensation procedure, in the limiting case of azimuthal symmetry for both the beam distribution and the beamline elements, will produce a minima in the radial emittance (ε_r) but will not affect the angular emittance (ε_L), which is significantly larger in the 'flat' beam than in the 'round' beam.

Laser Pulse Shaping and Thermal Emittance

As part of the design process, the temporal profile of the photocathode excitation laser pulse was varied and the beamline was optimized for transport of the 'round' beam between the cathode and the linac exit. The laser produced a nominal 1nC in the beam core comprising the flat-top region. The beam had an assumed 0.5mm rms spot size at the cathode with thermal emittance of 0.6mm. The ASTRA results are shown in Table 1. Lower emittance was achieved at every stage by going to longer pulses thereby reducing the local space charge forces. For given flat-top durations, however, lower projected emittances within the core were obtained with the shorter rise- and fall-times.

Table 1. Emittances of 'round' beams along the injector.

		Gun		GTL		Linac	
Rise (ps)	Flat (ps)	ε_{2D}	ε_r	ε_{2D}	ε_r	ε_{2D}	ε_r
2.5	20	2.4	2.2	1.6	1.5	1.8	1.4
	25	1.8	1.5	1.2	1.1	1.1	0.84
	30	1.4	1.1	0.96	0.86	0.87	0.68
	35	1.1	0.84	0.88	0.80	0.80	0.69
5	25	2.0	1.7	1.4	1.3	1.2	0.99
	30	1.5	1.3	1.2	1.1	0.95	0.76
	35	1.2	0.95	0.95	0.85	0.82	0.64

Observation of the beam during low energy transport demonstrated that the beam self- and image-charge forces for an RMS spot size during photoemission of 0.5mm were capable of producing significant reduction in peak accelerating fields and nonlinearities in the longitudinal charge density profile. This deviation from uniformity along the nominal flat-top region limits the effectiveness of linear space charge emittance compensation techniques. An approximate balance between the thermal emittance contribution at larger beam spots and the loss of effectiveness of emittance compensation for smaller beam spots was found by choosing a 1mm RMS spot size as the optimum operating point.

ADAPTER AND MATCHING OPTICS

The adapter optics downstream from the linac serve to convert angular momentum carried by the 'flat' beam into a large x/y emittance ratio, with no coupling between transverse phase spaces. This section is entirely composed of skew quadrupoles. Following this lattice, a matching section serves to match the beta functions of both beam classes to the values required at the entrance to the first compressor arc.

Round-to-Flat Adapter Optics

The adapter lattice is composed of three fixed strength skew quadrupoles and four pulsed skew quadrupoles to tailor the lattice for each class of beam.

From linear coupling, azimuthally symmetric beams with finite angular momentum carry circular mode emittances given by $\varepsilon_{\pm} = \pm\langle L\rangle/2 + \sqrt{\varepsilon_r^2 + \langle L^2\rangle/4}$. In a suitable skew quad channel, these modes are converted to pure transverse emittances $\boldsymbol{\varepsilon}_x = \boldsymbol{\varepsilon}_+$, $\boldsymbol{\varepsilon}_y = \boldsymbol{\varepsilon}_-$. The adapter lattice has been optimized to decouple 'flat' beam while maintaining minimum asymmetry in the 'round' beam. The results of ASTRA simulations are shown in Figure 3. The 'flat' beam has been decoupled with x/y emittances 19/0.18πmm-mrad and. The 'round' beam emerges uncoupled but slightly asymmetric with x/y emittances 1.4/1.1 π mm-mrad. In both cases the 4D emittances remain invariant. The small asymmetry in the 'round' beam emittance is a result of nonzero RMS canonical angular momentum induced at the cathode

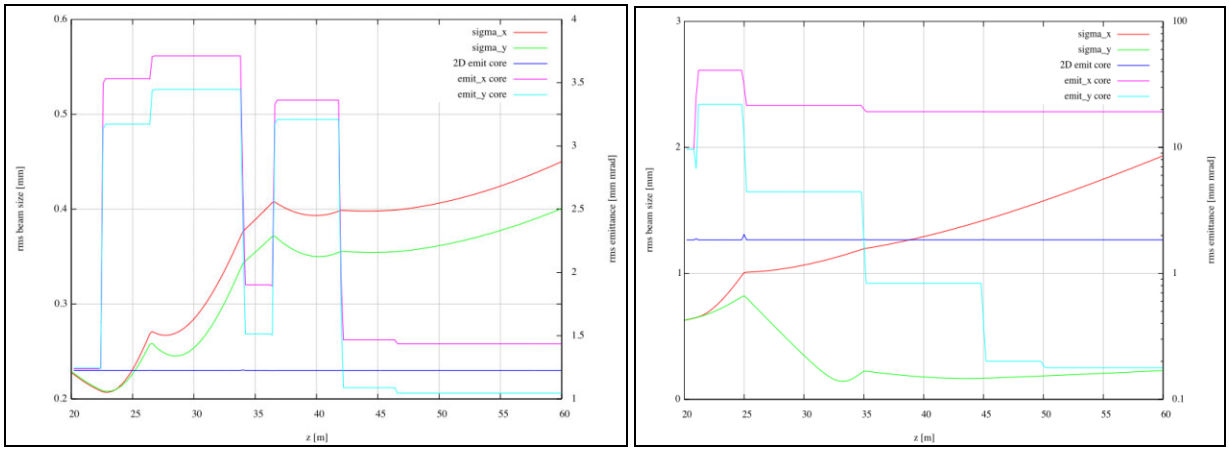

Figure 3. Core emittances and spot sizes in the adapter for the 'round' beam (left) and 'flat' beam (right).

from off-axis variation of the magnetic solenoid field.

Matching to the Compressor Arc

The matching lattice serves to match the beta functions of the different beam classes to the required values at the entrance to the compressor arc. The lattice is composed of three fixed strength normal quadrupoles and five pulsed normal quadrupoles. The two lattices were optimized with MAD 8. The Courant-Snyder parameters at the matching section entrance and the compressor entrance are listed in Table 2. The evolution of the parameters is shown in Figure 4.

Table 2. Courant-Snyder parameter values in the matching section.

Initial 'Round' Beam Parameters				
$\gamma\varepsilon_x$	1.4π mm-mrad		$\gamma\varepsilon_y$	1.0π mm-mrad
β_x	38 m		β_y	38 m
α_x	-0.42		α_y	-0.42
Initial 'Flat' Beam Parameters				
$\gamma\varepsilon_x$	19.π mm-mrad		$\gamma\varepsilon_y$	0.18π mm-mrad
β_x	58 m		β_y	58 m
α_x	-1.2		α_y	-1.2
Required Parameters At Compressor Arc Entrance				
β_x	0.59 m		β_y	2.6 m
α_x	0.64		α_y	-1.3

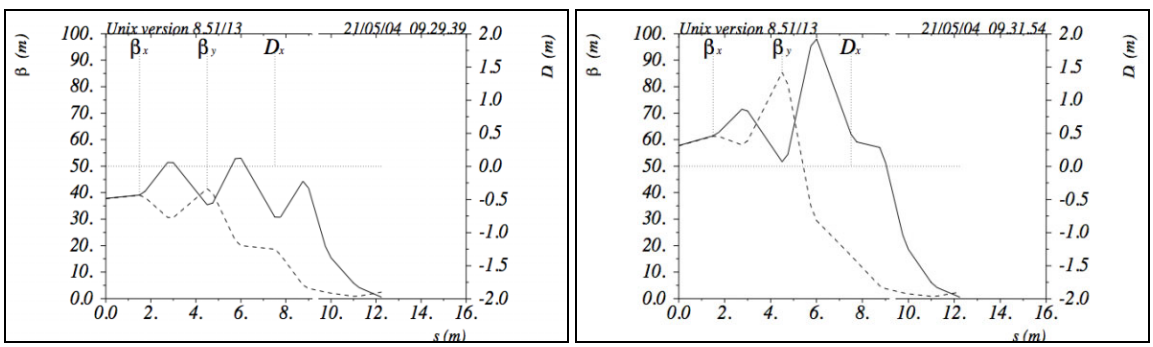

Figure 4. Beta functions for the 'round' beam (left) and 'flat' beam (right) in the 'matching' section.

REFERENCES

[1] J. Corlett, *et. al.*, "LUX – A Recirculating Linac-Based Facility For Ultrafast X-Ray Science", *Proc. 9th Euro. Part. Accel. Conf.*, Lucerne, 2004.

[2] S. Lidia, *et. al.*, "An Injector For The Proposed Berkeley Ultrafast X-Ray Light Source", *Proc. 2003 Part. Accel. Conf.*, Portland, 2003.

[3] D. Edwards, et. al., "The Flat Beam Experiment At The FNAL Photoinjector", *Proc. XXth Int'l. Linac Conf.*, Monterey, 2000.

[4] J. Staples, *et. al.*, "The LBNL Femtosource 10 kHz Photoinjector", *Proc. 2003 Part. Accel. Conf.*, Portland, 2003.

[5] K. Flöttmann, www.desy.de/mpyflo/Astra.

[6] W.S. Graves, "Measurement Of Thermal Emittance For A Copper Photocathode", *Proc. 2001 Part. Accel. Conf.*, Chicago, 2001.